Multi-loop Sliding-Mode Control for a Battery Charger Using a Quadratic Buck Converter

Oswaldo López-Santos*, F. Flores-Bahamonde†, C. A. Torres-Pinzón‡, Reham Haroun*, Hugo Valderrama-Blavi*, Juan A. Garriga§ and Luis Martínez-Salamero*

* *Group of Automatic Control and Industrial Electronics*, Rovira i Virgili University, Tarragona, Spain
† *Energy Transformation Center*, Faculty of Enigineering, Universidad Andres Bello, Chile
‡ *Faculty of Electronic Engineering*, Universidad Santo Tomás, Colombia
§ *Department of Computer Science and Industrial Engineering*, University of Lleida, Lleida, Spain.
email: freddy.flores@unab.cl

***Abstract*—In this paper, the quadratic buck converter (QBC) is proposed as competitive alternative to implement a battery charger. Since, QBC is a high order system, the required control is designed to follow the conventional constant-current constant-voltage regime by means of three loops. Namely, i) an inner-loop operating in sliding mode to control the current of the closest inductor to the input port providing the properly stability of the system, ii) a first outer loop designed to regulate the battery voltage providing the reference of the inner loop, and finally iii) a second outer loop to regulate the battery current modifying the reference of the voltage loop. Proportional Integral (PI) controllers are used in both outer loops. Simulation results are presented validating the theoretical study.**

***Index Terms*—Sliding Mode Control, Quadratic Buck Converter, Battery charger**

I. Introduction

Battery energy storage is widely used in mobile systems operating with a certain temporary energy autonomy such as cell phones, drones and electric vehicles (EVs) [1]- [2]. For these applications, the batteries are replenished using battery chargers which are composed of a unidirectional power converter and its control system. The main function of these chargers is to provide the necessary energy to the batteries favoring a good utilization to increase its lifetime. The voltage and power levels of the chargers depend on the application and are defined by the size of the battery array and the expected charging time. For example, battery chargers for the electric vehicle application can provide between 100 and 800 V with an output power of up to 350 kW. Depending on the relation between the battery capacity and the transferred power, the charging time varies from fractions of an hour to several hours [3]- [4]. The advances increasing the maximum output power of the chargers in the market has allowed to replenish the battery of an EV in less than fifteen minutes. This technology refers to the so called fast-chargers and ultrafast-chargers.

Battery chargers can be classified as isolated or non-isolated and can be powered by alternating current (AC chargers) or direct current (DC chargers). The AC chargers normally are composed of two power conversion stages, one performing rectification ensuring a unitary power factor and other performing regulation of the DC output voltage and current. In turn, the DC chargers can be implemented using a single stage of DC-DC conversion which is fed by a primary system providing a regulated DC output. The selection of the adequate DC-DC power converter in both cases (output stage) depends on the constraints of the application mainly related with the input and output voltage ranges, the rated power and the requirement of galvanic isolation. For instance, the quadratic buck converter (QBC) may be a suitable candidate in applications where: a) the DC input voltage is various times higher than the battery array voltage; b) galvanic isolation is not mandatory because it is provided by a previous conversion stage; and c) the required output current is high. The main reason is the ability of this converter to provide a high step-up current gain without the need of transformers [5]- [6].

The energy processed by a battery charger is transferred from a primary power source to the battery following a charging method. Most of the methods perform the charge in a sequence of stages in which the charger applies a constant DC current or a constant DC voltage. The classical method consist in applying a constant current to the battery while it reaches a predefined voltage level and then apply that voltage until the battery is completely charged. This method is well known as the constant current – constant voltage (CC-CV) method [7]. Other methods can use multiple stages of constant current with increasing references like in the case of [8] and [9].

Sliding mode control has been used in power converters proving to be a superior alternative in terms of simplicity of implementation, speed of response and robustness [10]–[12]. This type of control can be applied using nested loops (multi-loop control) in which an inner loop ensures operation in a sliding mode while an outer loop impose regulation or tracking in a variable of interest [13] - [14]. A key aspect in the multi-loop implementation is the choice of the variables involved in

This work has been partially sponsored by the Spanish Ministerio de Ciencia e Innovación under grants MSCA IF EF-ST 2020 / PCI2021-122066-2B and PID2019-111443RB-I00, and partially by the Chilean Agencia Nacional de Investigación y Desarrollo (ANID) through projects FONDECYT Iniciación 11220863 and SERC Chile (CONICYT/FONDAP/15110019) as well as by Universidad Santo Tomás through grant project no. BOG-2023-AI015.

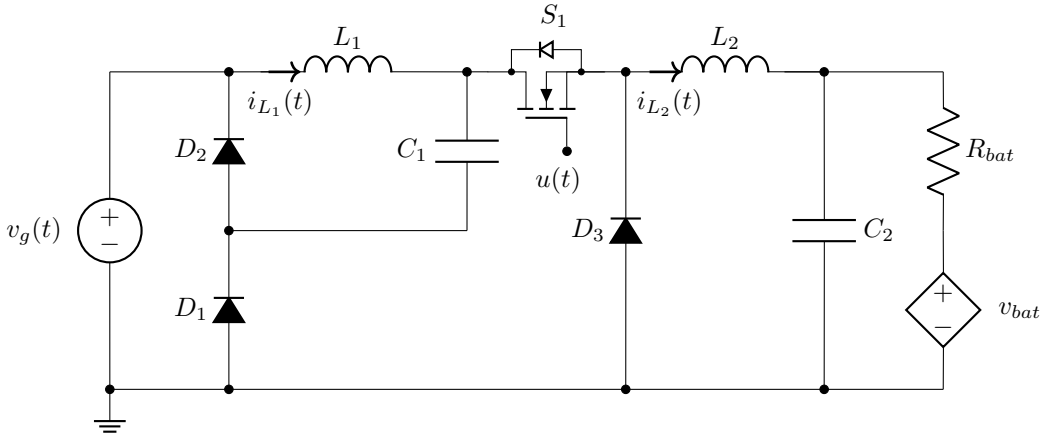

Fig. 1: Schematic circuit diagram of a quadratic buck converter feeding a battery type load.

the sliding surface of the inner loop since the stability depends on it. As it can be verified in [15], [16] and [17], despite the complexity of the power converter, the use of a single inductor current in the sliding surface is a simple and effective choice. Also, in [6] although the use of the current of an inductor in the sliding surface does not allow a direct stabilization of the converter because the constant power nature of the load, it facilitates the stabilization by the outer loop. Conventionally, the outer loop of the control system is configured using a proportional-integral (PI) controller which offers the solution with the best cost-benefit trade-off.

This paper proposes a multi-loop control method based on sliding mode to control the QBC as a battery charger. The proposal involves an inner loop of sliding mode control and two nested outer regulation loops to perform the above mentioned CC-CV charging method. The sliding surface of the inner loop involves only the inductor current closer to the input port of the converter. The first outer loop implemented using a PI controller regulates the battery voltage at a reference value which is fixed for the constant voltage interval. During the constant current interval, the more external outer loop also implemented using a PI controller modifies the voltage reference in order to impose the charging current limitation. The synthesis of the controllers is assisted by the Control Systems Designer of MATLAB considering the basic fundamentals for design of cascade controllers. The main contributions of this paper are: 1) the theoretical analysis of the proposed control applied to the quadratic buck converter feeding a battery, which is represented by a voltage source in series with a resistor, thus extending the work presented in [6], and 2) the application of the proposed multi-loop controller for the quadratic buck converter in the battery charging application extending the work reported in [17]. The rest of the paper is organized as follows: Section II presents the circuit analysis used to derive the model of the quadratic buck converter. After that, section III presents the theoretical analysis of the inner current control loop developed using sliding mode control. Section IV develops the synthesis of the outer loops to impose the desired CC-CV battery charging regime. Finally, simulation results are presented in Section V and conclusions are presented in Section VI.

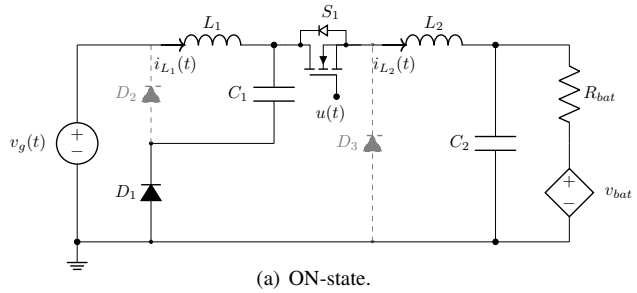

(a) ON-state.

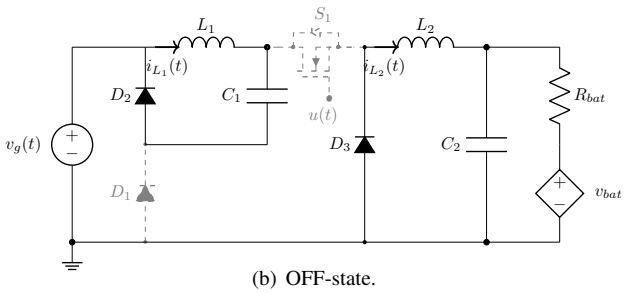

(b) OFF-state.

Fig. 2: Quadratic buck circuit configurations.

II. Switched-model of the QBC

The electrical circuit of the QBC proposed for battery charging is shown in Fig. 1. As it can be noted, the circuit is composed by the inductors L_1 and L_2, the capacitors C_1 and C_2, the diodes D_1, D_2 and D_3, and the controlled switch S_1 which is governed by the control signal $u(t)$. As stated, this circuit provides a wider conversion ratio than the conventional buck converter, since the dc gain between the output voltage and the input voltage is a quadratic function, described by

$$\frac{V_{C_2}}{V_g} = D^2 \tag{1}$$

where V_{C_2} and V_g are the average values of the output and input voltage, and D is the duty cycle of the converter which is defined as the average value of the control signal $u(t)$. As can be observed, the converter is also connected to a battery modeled as the controlled voltage source v_{bat} connected in series with the resistance R_{bat}. Although the resistance R_{bat} slightly varies during the charging process, in the subsequent analysis it is considered constant.

The QBC has only one active switch to perform the voltage conversion and its operation is equivalent to have two cascaded buck converters sharing the same control signal. Thus, through the control signal $u(t) = \{0, 1\}$ two configurations are obtained for operation in continuous conduction mode (CCM). Figure 2(a) shows the ON−state configuration associated to $u(t) = 1$, and Figure 2(b) the OFF−state configuration, corresponding to $u(t) = 0$.

The state vector of the converter is given in (2). Operating in CCM, the dynamics of the QBC can be modelled by means of the bilinear system equation (3).

$$x(t) = \begin{bmatrix} i_{L_1}(t) & v_{C_1}(t) & i_{L_2}(t) & v_{C_2}(t) \end{bmatrix}^T \tag{2}$$

$$\begin{aligned} \frac{di_{L_1}}{dt} &= -\frac{v_{C_1}}{L_1} + \frac{v_g}{L_1}u \\ \frac{dv_{C_1}}{dt} &= \frac{i_{L_1}}{C_1} - \frac{i_{L_2}}{C_1}u \\ \frac{di_{L_2}}{dt} &= \frac{v_{C_1}}{L_2}u - \frac{v_{C_2}}{L_2} \\ \frac{dv_{C_2}}{dt} &= \frac{i_{L_2}}{C_2} - \frac{\left(v_{C_2} - v_{bat}\right)}{R_{bat}C_2} \end{aligned} \tag{3}$$

III. Sliding mode control

The switching surface considered in this application is defined as $S(x) = i_{L_1} - k(t)$, where $k(t)$ is provided by an outer control loop. Introducing the invariance conditions $S(\mathbf{x}) = 0$ and $\frac{dS(\mathbf{x})}{dt} = 0$ in (4) results in the equivalent control $u_{eq}(\mathbf{x})$ bounded as follows:

$$0 < \left[u_{eq}(\mathbf{x}) = \frac{L_1 \frac{dk}{dt} + v_{C_1}}{V_g} \right] < 1 \tag{4}$$

Now, substituting u by $u_{eq}(\mathbf{x})$ in (3) results in the following ideal sliding dynamics:

$$\begin{aligned} \frac{dv_{C_1}}{dt} &= \frac{k}{C_1} - \frac{L_1}{C_1}\frac{i_{L_2}}{v_g}\frac{dk}{dt} - \frac{i_{L_2}}{C_1}\frac{v_{C_1}}{v_g} &&= g_1(\mathbf{x}) \\ \frac{di_{L_2}}{dt} &= \frac{L_1}{L_2}\frac{v_{C_1}}{v_g}\frac{dk}{dt} + \frac{v_{C_1}^2}{L_2 v_g} - \frac{v_{C_2}}{L_2} &&= g_2(\mathbf{x}) \\ \frac{dv_{C_2}}{dt} &= \frac{i_{L_2}}{C_2} - \frac{\left(v_{C_2} - v_{bat}\right)}{R_{bat}C_2} &&= g_3(\mathbf{x}) \end{aligned} \tag{5}$$

The coordinates of the equilibrium point are given by:

$$x^* = \left[i_{L_1}^*, v_{C_1}^*, i_{L_2}^*, v_{C_2}^* \right]^T \tag{6}$$

where $i_{L_1}^* = k^*$, $v_{C_1}^* = \sqrt{V_{bat}V_g}$, $i_{L_2}^* = k^*\sqrt{\frac{V_g}{V_{bat}}}$ and $v_{C_2}^* = V_o = \frac{\sqrt{V_{bat}^3} + k^* R_{bat}\sqrt{V_g}}{\sqrt{V_{bat}}}$.

Taking into account the equations (4), (5), and (6), the ideal sliding dynamics can be linearized as:

$$\begin{aligned} \frac{d\widetilde{v}_{C_1}}{dt} &= a_{11}\widetilde{v}_{C_1} + a_{12}\widetilde{i}_{L_2} + a_{13}\widetilde{v}_{C_2} + b_{11}\widetilde{k} + c_{11}\frac{d\widetilde{k}}{dt} \\ \frac{d\widetilde{i}_{L_2}}{dt} &= a_{22}\widetilde{v}_{C_1} + a_{21}\widetilde{i}_{L_2} + a_{23}\widetilde{v}_{C_2} + b_{21}\widetilde{k} + c_{21}\frac{d\widetilde{k}}{dt} \\ \frac{d\widetilde{v}_{C_2}}{dt} &= a_{33}\widetilde{v}_{C_1} + a_{32}\widetilde{i}_{L_2} + a_{33}\widetilde{v}_{C_2} + b_{31}\widetilde{k} + c_{31}\frac{d\widetilde{k}}{dt} \end{aligned} \tag{7}$$

The parameters a_{ij}, b_{ij}, c_{ij}, $(i, j \in \{1, 2, 3\})$ are defined as:

$$\begin{aligned} a_{11} &= -\frac{k^*}{C_1\sqrt{V_g V_{bat}}} & a_{12} &= -\frac{1}{C_1}\sqrt{\frac{V_{bat}}{V_g}} \\ a_{13} &= 0 \\ b_{11} &= \frac{1}{C_1} & c_{11} &= -\frac{L_1}{C_1}\frac{k^*}{\sqrt{V_g V_{bat}}} \\ a_{21} &= \frac{2}{L_2}\sqrt{\frac{V_{bat}}{V_g}} & a_{22} &= 0 \\ a_{23} &= -\frac{1}{L_2} \\ b_{21} &= 0 & c_{21} &= \frac{L_1}{L_2}\sqrt{\frac{V_{bat}}{V_g}} \\ a_{31} &= 0 & a_{32} &= \frac{1}{C_2} \\ a_{33} &= -\frac{1}{R_{bat}C_2} \\ b_{31} &= 0 & c_{31} &= 0 \end{aligned}$$

By applying the Laplace transform to (7), the transfer function given by (8) is obtained:

$$G_{vk}(s) = \frac{\tilde{v}_{C_2}(s)}{\tilde{k}(s)} = \frac{\beta_2 s^2 + \beta_1 s + \beta_0}{s^3 + \alpha_2 s^2 + \alpha_1 s + \alpha_0} \tag{8}$$

where

$$\begin{aligned} \beta_2 &= a_{32}c_{21} & \beta_1 &= a_{32}\left(c_{11}a_{21} - a_{11}c_{21}\right) \\ \beta_0 &= a_{32}b_{11}a_{21} & \alpha_2 &= -a_{11} - a_{33} \\ \alpha_1 &= \left(a_{11}a_{33} - a_{23}a_{32} - a_{12}a_{21}\right) \\ \alpha_0 &= \left(a_{11}a_{23}a_{32} + a_{12}a_{21}a_{33}\right) \end{aligned}$$

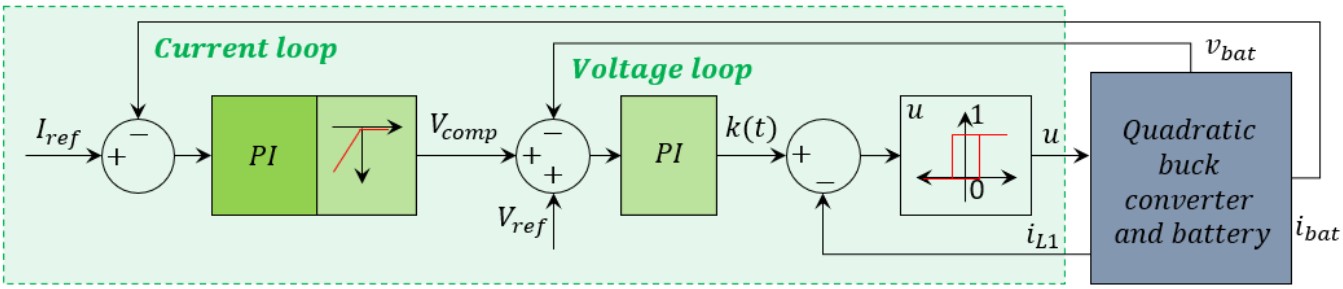

Fig. 3: Proposed battery charger control architecture.

IV. Battery charging control

A. Control architecture and charging method

The control scheme depicted in Fig. 3 is proposed to apply the CC-CV charging method based on sliding mode control. This is achieved by using an inner loop based on a sliding mode control and two nested outer loops regulating the voltage and current of the battery. Specifically, the sliding mode controller acting on the inductor current i_{L1} has been implemented by means of an hysteresis comparator which enforces a finite switching frequency. The reference of this control loop, $k(t)$, is given by a first outer loop, which is composed of a classical PI compensator that acts minimizing the output voltage error. The reference of this loop is obtained as the sum of the desired voltage for the CV interval denoted as V_{ref} and the contribution of the most outer loop regulating the current of the battery and denoted as V_{comp}. Since this current is a function of the output voltage and the instantaneous static impedance of the battery, the current limitation during the CC interval can be provided by another PI compensator acting on the battery current error and tracking the reference I_{ref}. As can be observed in the scheme of Fig. 3, the current error is saturated at zero, thus, the contribution of this loop through V_{comp} takes only negative values.

B. Synthesis of the controllers

In order to design the PI controllers of the respective nested loops, the parameters of the converter are described in Table I. As a result, the parameters of the third order transfer function of expression (8) become:

$$\beta_2 = 13.298 \times 10^3 \qquad \beta_1 = -1.052 \times 10^6$$
$$\beta_0 = 73.879 \times 10^9 \qquad \alpha_2 = 100 \times 10^3$$
$$\alpha_1 = 43.705 \times 10^6$$
$$\alpha_0 = 248.25 \times 10^9$$

In this way, using the output to control transfer function and following a conventional design method, the PI controllers of the first and second outer loops can be designed. The synthesis of these controllers is assisted by the Control Systems Designer of MATLAB© by using the root locus design method. The PI controllers follow the form:

TABLE I: System parameters

Symbol	Parameter	Value
P	Rated power	540 W
V_o	Output voltage	40 -54 V
V_{bat}	Battery voltage	40 -54 V
I_{bat}	Output current	10 A
V_g	Input voltage	380 V
R_{bat}	Battery resistance	0.1 Ω
L_1	Input inductor	1.2 mH
L_2	Output inductor	0.3 mH
C_1	Input capacitor	0.3 mF
C_2	output capacitor	0.1 mF

$$G_{cn}(s) = \frac{K_{pn}s + K_{in}}{s} \tag{9}$$

where $n = \{i, v\}$ indicates the voltage or current loop, respectively.

The specifications for the voltage regulation loop are a settling time of 0.1 s without overshoot. The transfer function used for the design is $G_{vk}(s)$ (Expression (8)). Thus, the closed loop transfer function of the voltage regulation loop is obtained as follows:

$$G_{vbat}(s) = \frac{G_{vk}(s)G_{cv}(s)}{1 + G_{vk}(s)G_{cv}(s)} \tag{10}$$

The gains of the voltage regulation loop were obtained as $K_{pv} = 0.34$ and $K_{iv} = 265.78$. Considering that the more outer loop needs to be at least ten times slower than the subsequent nested loop to satisfy conventional constraints of cascade controllers design, the specifications for the current regulation loop are a settling time of 1 s without overshoot. The output voltage of the converter is applied to the battery model in which the current is defined by:

$$i_{bat} = \frac{v_{C_2} - v_{bat}}{R_{bat}} \tag{11}$$

Then, the transfer function used for the design is as follows:

$$G_{iv}(s) = \frac{G_{vbat}(s)}{R_{bat}} \tag{12}$$

The gains of the current regulation loop were obtained as $K_{pi} = 0.0034$ and $K_{ii} = 0.6$. The closed loop transfer function of the current regulation loop is obtained as follows:

$$G_{ibat}(s) = \frac{G_{iv}(s)G_{ci}(s)}{1 + G_{iv}(s)G_{ci}(s)} \tag{13}$$

It is worth to mention that although the order of the resulting dynamics of this control loop is five, it is enforced to approximately have the dynamics of a first order system.

V. Simulation Results

The power converter circuit and battery models have been simulated using PSIM© software according to the circuit scheme described in Fig. 1. The first simulation has been performed in order to verify the stable operation of the converter. The parameters of the converter defined in Table I are used. The sliding mode controller is implemented by means of a hysteresis comparator composed of two simple comparators and one S-R flip-flop and defined for a band of $\pm$ 0.5 A. Using this implementation, the switching frequency varies depending of the operation point but is constrained to dozens of kHz. Measurements are acquired when the output voltage is 54 V and a value of 53 V in reached in the variable v_{bat} of the battery model. Fig. 4 shows some high frequency cycles of the converter variables detailing the ripples and average values.

The second simulated scenario simulated has been designed to verify the correct operation of the proposed control, i.e., following the CC-CV charging method. The battery model considers a capacity of 2.5 Ah, and the internal voltage v_{bat} evolves as a function of the state of charge from 0 % to 100 %. As it can be seen in Fig. 5, in the first interval, the system operates in the CC interval following a set-point of 10 A provided by the action of the outermost control loop. During this interval of approximately 850 s, the voltage applied to the battery increases from 42 V until it reaches the voltage reference value of 54 V. Thereafter, this voltage reference is maintained constant until the battery is fully charged while the current decreases exponentially until zero. The last interval has a duration of about 300 s.

VI. Conclusions

In this paper, the quadratic buck converter has been studied in the application of battery charging. Due to the higher order of the system, a multi-loop controller using three nested loops has been proposed involving one sliding mode current controller and two conventional PI controllers. The selected sliding surface uses the inearest nductor current to the input port because the individual selection of the other variables leads to an unstable behavior and the use of a linear combination of more than one variable implies added complexity and does not improve the achieved performance. Simulated results show that the studied converter operates properly following the conventional CC-CV charging method by using the proposed control scheme. A laboratory prototype is under implementation in order to provide experimental validation.

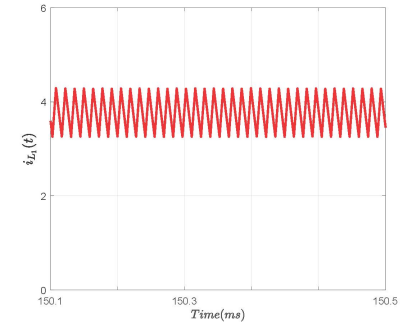

(a) i_{L_1}

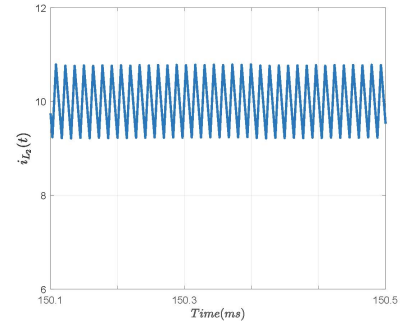

(b) i_{L_2}

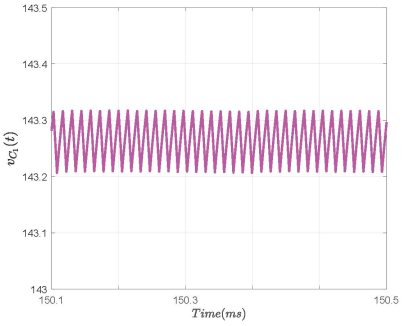

(c) v_{C_1}

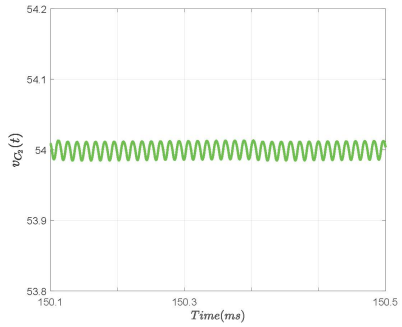

(d) v_{C_2}

Fig. 4: Steady-state current and voltage waveforms.

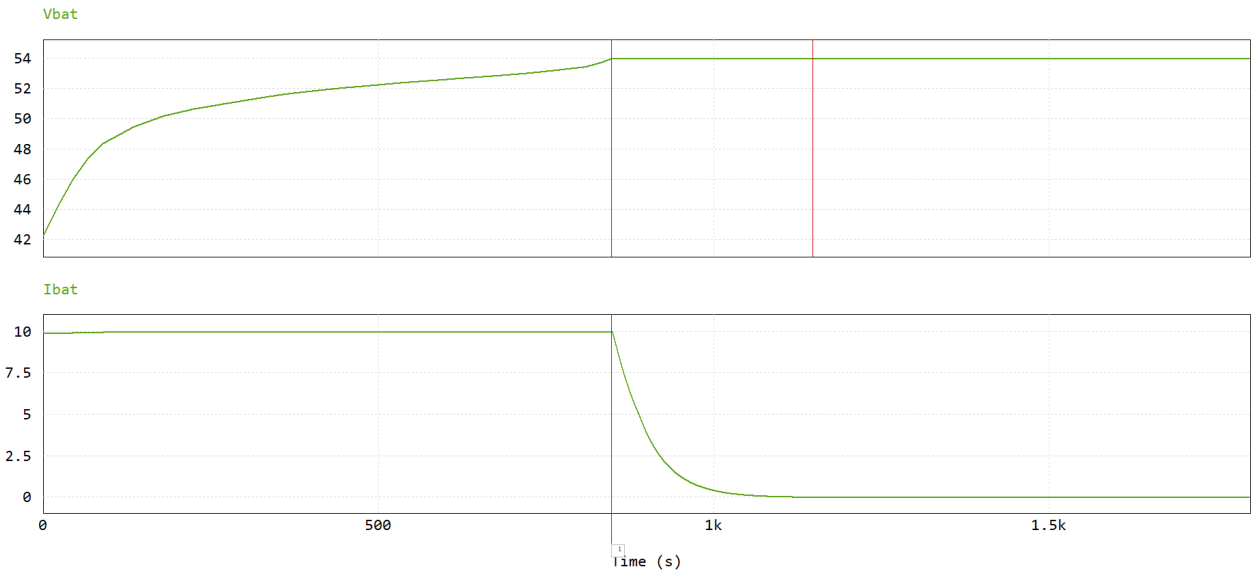

Fig. 5: Battery voltage and current during a complete CC-CV changing cycle.

Further research contemplates the study of the interleaving operation [18] of this converter for battery charging.

REFERENCES

[1] J. Cao and A. Emadi, "Batteries need electronics," *IEEE Ind. Electron. Mag.*, vol. 5, no. 1, pp. 27–35, Mar. 2011.

[2] K. Pham, J. Leuchter, R. Bystricky, M. Andrle, N. Pham, and V. Pham, "The study of electrical energy power supply system for uavs based on the energy storage technology," *Aerospace*, vol. 9, no. 9, pp. 500–529, Sep. 2022.

[3] M. Safayatullah, M. Elrais, S. Ghosh, R. Rezaii, and I. Batarseh, "A comprehensive review of power converter topologies and control methods for electric vehicle fast charging applications," *IEEE Access*, vol. 10, pp. 40 753–40 793, 2022.

[4] S. Rivera, S. Kouro, S. Vazquez, S. M. Goetz, R. Lizana, and E. Romero-Cadaval, "Electric vehicle charging infrastructure: From grid to battery," *IEEE Ind. Electron. Mag.*, vol. 15, no. 2, pp. 37–51, Jun. 2021.

[5] J. Morales-Saldana, J. Leyva-Ramos, E. Carbajal-Gutierrez, and M. Ortiz-Lopez, "Average current-mode control scheme for a quadratic buck converter with a single switch," *IEEE Trans. Power Electron.*, vol. 23, no. 1, pp. 485–490, Jan. 2008.

[6] C. Torres-Pinzón, F. Flores-Bahamonde, J. Garriga-Castillo, H. Valderrama-Blavi, R. Haroun, and L. Martínez-Salamero, "Sliding-mode control of a quadratic buck converter with constant power load," *IEEE Access*, vol. 10, pp. 71 837–71 852, 2022.

[7] B.-Y. Chen and Y.-S. Lai, "New digital-controlled technique for battery charger with constant current and voltage control without current feedback," *IEEE Trans. Ind. Electron.*, vol. 59, no. 3, pp. 1545–1553, Mar. 2012.

[8] J. Deng, S. Li, S. Hu, C. Mi, and R. Ma, "Design methodology of llc resonant converters for electric vehicle battery chargers," *IEEE Trans. Vehicular Technol.*, vol. 63, no. 4, pp. 1581–1592, May 2014.

[9] D. Lyu, T. Soeiro, and P. Bauer, "Impacts of different charging strategies on the electric vehicle battery charger circuit using phase-shift full-bridge converter," *in Proc. IEEE 19th Intl. Power Electron. Motion Control Conf. (PEMC)*, 2021.

[10] S.-C. Tan, Y. Lai, and C. Tse, "General design issues of sliding-mode controllers in dc–dc converters," *IEEE Trans. Ind. Electron.*, vol. 55, no. 3, pp. 1160–1174, Mar. 2008.

[11] L. Martinez-Salamero, A. Cid-Pastor, A. ElAroudi, R. Giral, J. Calvente, and G. Ruiz-Magaz, "Sliding-mode control of dc-dc switching converters," *Proceedings of IFAC World Conference, Milano, Italy*, vol. 44, no. 1, pp. 1910–1916, 2011.

[12] D. Zambrano-Prada, A. El Aroudi, L. Vázquez-Seisdedos, and L. Martinez-Salamero, "Polynomial sliding surfaces to control a boost converter with constant power load," *IEEE Trans. Circuits Syst. I: Reg. Papers*, vol. 70, no. 1, pp. 530–543, Jan. 2023.

[13] E. Vidal-Idiarte, C. Carrejo, J. Calvente, and L. Martínez-Salamero, "Two-loop digital sliding mode control of dc–dc power converters based on predictive interpolation," *IEEE Trans. Ind. Electron.*, vol. 58, no. 6, pp. 2491–2501, June 2011.

[14] O. Lopez-Santos, G. Garcia, L. Martinez-Salamero, J. Avila-Martinez, and L. Seguier, "Non-linear control of the output stage of a solar microinverter," *Intl. J. Control*, vol. 90, no. 1, pp. 90–109, 2017.

[15] O. Lopez-Santos, L. Martinez-Salamero, G. Garcia, H. Valderrama-Blavi, and T. Sierra-Polanco, "Robust sliding-mode control design for a voltage regulated quadratic boost converter," *IEEE Trans. Power Electron.*, vol. 30, no. 4, pp. 2313–2327, Apr. 2015.

[16] Z. Chen, "Pi and sliding mode control of a cuk converter," *IEEE Trans. Power Electron.*, vol. 27, no. 8, pp. 3695–3703, Aug. 2012.

[17] O. Lopez-Santos, D. Zambrano Prada, Y. Aldana-Rodriguez, H. Esquivel-Cabeza, G. Garcia, and L. Martinez-Salamero, "Control of a bidirectional cuk converter providing charge/discharge of a battery array integrated in dc buses of microgrids," *Applied Computer Sciences in Engineering. WEA 2017. Commun. Comput. Inf. Sci.*, vol. 742, pp. 495–507, Aug. 2017.

[18] S. Ozeri, D. Shmilovitz, S. Singer, and L. Martinez-Salamero, "The mathematical foundation of distributed interleaved systems," *IEEE Trans. Circuits Syst. I: Reg. Papers*, vol. 54, no. 3, pp. 610–619, Mar. 2007.